Title	Cytotoxicity and antimicrobial activity of triorganotin(IV) complexes of phenylcyanamide prepared by sonochemical synthesis
Author(s)	Tabrizi, Leila; McArdle, Patrick; Erxleben, Andrea; Chiniforoshan, Hossein
Publication Date	2015-09-25
Publication Information	Tabrizi, Leila, McArdle, Patrick, Erxleben, Andrea, & Chiniforoshan, Hossein. (2015). Cytotoxicity and antimicrobial activity of triorganotin(IV) complexes of phenylcyanamide prepared by sonochemical synthesis. Inorganica Chimica Acta, 438, 94-104. doi: https://doi.org/10.1016/j.ica.2015.09.011
Publisher	Elsevier
Link to publisher's version	https://doi.org/10.1016/j.ica.2015.09.011
Item record	http://hdl.handle.net/10379/6543
DOI	http://dx.doi.org/10.1016/j.ica.2015.09.011

Cytotoxicity and antimicrobial activity of triorganotin(IV) complexes of phenylcyanamide prepared by sonochemical synthesis

Leila Tabrizi [a,b], Patrick McArdle [b], Andrea Erxleben [b,*], Hossein Chiniforoshan [a,*]

[a] Department of Chemistry, Isfahan University of Technology, Isfahan 84156-83111, Iran

[b] School of Chemistry, National University of Ireland Galway, University Road, Galway, Ireland

[a,*]Corresponding author: H. Chiniforoshan; Email: Chinif@cc.iut.ac.ir
Tel: +983133913261; fax: +983133912350

[b,*]Corresponding author: Andrea Erxleben; Email: andrea.erxleben@nuigalway.ie
Tel: +353(0)91-492483; fax: +353(0)91-495576

Abbreviations:

DNA, deoxyribonucleic acid; CT-DNA, calf thymus DNA; BSA, bovine serum albumin; HSA, human serum albumin; EB, ethidium bromide; IC_{50}, half maximal inhibitory concentration; SV, Stern–Volmer; bpH_2, 4,4′-dicyanamidobiphenyl; 4-NO_2pcyd, 4-nitrophenylcyanamide; FT-IR, Fourier transform infrared spectroscopy; UV-Vis, ultraviolet visible; NMR, nuclear magnetic resonance; calc., calculated; DMSO, dimethyl sulfoxide; SEM, scanning electron microscopy; TEM, transmission electron microscopy.

Abstract

This article describes the synthesis and characterization of novel triorganotin(IV) complexes and their potential medicinal applications. Triorganotin(IV) complexes with formulas $[(SnMe_3)_2(\mu\text{-bp})(H_2O)_2]$, **1**, and $[(SnMe_3)(4\text{-}NO_2pcyd)]$, **2**, (Me: methyl, bpH_2: 4,4′-dicyanamidobiphenyl and $4\text{-}NO_2pcyd$: 4-nitrophenylcyanamide) have been synthesized *via* a sonochemical process and characterized using multinuclear NMR (^{1}H, ^{13}C and ^{119}Sn), Mössbauer spectroscopy, elemental analysis, scanning electron microscopy (SEM) and transmission electron microscopy (TEM). Compounds **1** and **2** were evaluated for their DNA/protein binding with calf thymus DNA (CT-DNA) and bovine serum albumin (BSA), respectively. The in vitro cytotoxicity of **1** and **2** was examined against A549, Du145, HeLa and MCF-7 cancer cell lines. For **1**, a promising growth inhibitory effect against HeLa cells was observed that is slightly higher than that of cisplatin. Moreover, the antimicrobial activity of **1** and **2** against different strains of pathogenic bacteria and fungi were tested. The free radical scavenging ability (OH, NO) of **1** and **2** was assessed.

Keywords: Triorganotin phenylcyanamide; DNA binding; BSA binding; Antioxidant activity; Cytotoxicity.

1. Introduction

Nanomaterials have unique properties in material science and biology. The unique properties and efficacy of nanoparticles arise from a diversity of features, including the similar size of nanomaterials and biomolecules such as proteins and nucleic acids. Furthermore, useful properties can be included into the design of the nanoparticles for manipulation or detection of biological structures and systems [1].

The application of metal complexes in the treatment of various illnesses is an expanding area in medicinal chemistry [2]. Organotin(IV) compounds have been attracting attention in recent years because of their antitumor properties. The antitumor properties of organotin coordination compounds are significantly influenced by their structure. The binding ability of organotin compounds towards target DNA depends on the coordination number and nature of groups bonded to the central tin atom [3-7].

Nitrogen containing organic compounds and their metal complexes have an extensive range of biological properties such as antitumor, antibacterial, antifungal and antiviral activities [8-16]. Phenylcyanamide ligands (pcyd) and their complexes are interesting and practically unexplored with regard to their biological behaviour [17,18]. The extensive π conjugation between the cyanamide group and the phenyl ring provides an energetically favorable means by which a metal ion can couple into a conjugated organic π system [19-21]. Towards this aim, several complexes of phenylcyanamide ligands with transition metals have been synthesized and the electronic properties of the cyanamide group, especially its large π-conjugated system, have been investigated [22-34].

Sonochemistry has been rapidly developed in recent years due to its potential in environmental applications [35]. Moreover, the economic advantages of ultrasound in practical scale-up has already been well established in the food industry. In general, as a part of a young and interesting scientific area, the application of ultrasound for general

environmental and green technology reasons has a promising future in chemical processing. In contrast to classical methods which often require harsh conditions and have low energy efficiency ultrasound is considered to be an important green chemistry tool which provides important waste minimization and energy conservation [36].

In our group Au nanowires with 4,4′-dicyanamidobiphenyl have recently been synthesized and used in the fabrication of gas sensors to detect low concentrations of CO at room temperature [26]. In a continuation of our work on phenylcyanamide ligands we now report the sonochemical synthesis of triorganotin(IV) complexes with the formulas [$(SnMe_3)_2$(μ-bp)$(H_2O)_2$], **1**, [$(SnMe_3)$(4-NO_2pcyd)], **2**, (Me: methyl, bpH_2: 4,4′-dicyanamidobiphenyl and 4-NO_2pcyd: 4-nitrophenylcyanamide) (Scheme 1), their characterization and bioactivity. To our knowledge, tin complexes with phenylcyanamide ligands have not been reported before.

Scheme 1.

2. Experimental

2.1. Materials

All solvents were obtained from Sigma-Aldrich and used as received. The bpH_2 and 4-NO_2pcyd ligands were synthesized as previously reported [23,26]. All other reagents were commercially available and used as received.

2.2. Physical measurements

Fourier transform infrared spectra were recorded on a FT-IR JASCO FT-IR Jasco 680- Plus spectrometer in the region of 4000-400 cm^{-1} using KBr pellets. Fluorescence spectra were obtained using a Perkin-Elmer LS55 fluorescence spectrofluorometer. UV-visible (UV-Vis) spectra were recorded on a JASCO 7580 UV-Vis-NIR double-beam spectrophotometer using a quartz cell with a path length of 10 mm.^{1}H, ^{13}C {^{1}H} and ^{119}Sn spectra were recorded on a Bruker Avance ARX 400 (400 MHz) or a Bruker Avance III 600 (600 MHz) spectrometer in DMSO-d_6. Chemical shifts are quoted relative to external $SiMe_4$ (^{1}H, ^{13}C) and $SnMe_4$ (^{119}Sn).

^{119}Sn Mössbaurer spectra were obtained with a constant acceleration microprocessor controlled spectrometer (Cryoscopic Ltd., Oxford, UK); a barium stannate source was used at room temperature, and samples were packed in Perspex disks and cooled to 77 K. Isomer shift data are relative to SnO_2. Circular dichroism spectroscopy was taken on a Jasco J-715 spectropolarimeter at room temperature. Elemental analyses were performed using a PerkinElmer 2400 series II CHN/O elemental analyzer. Scanning electron microscopy (SEM) studies were performed with JEOL JSM 5600 and transmission electron microscopy (TEM) studies were performed with Tecnai 20 G^2 under 200 KV. ESI Mass Spectra were recorded with a Waters LCT Premier XE Spectrometer. The complexes were dissolved in DMSO and diluted with water (1% DMSO (v/v)).

2.3. Synthesis of organotin(IV) complexes

2.3.1. Synthesis of $[(SnMe_3)_2(\mu\text{-}bp)(H_2O)_2]$, 1

398 mg (2 mmol) trimethyltin chloride in water (10 mL) was added to 234 mg (1 mmol) of the ligand bpH_2 and 80 mg (2 mmol) NaOH in ethanol (10 mL). The reaction was carried out at room temperature with magnetic stirring which formed a homogeneous suspension. After stirring for about 60 min, the reaction mixture was irradiated with high-intensity ultrasound (SK1200 H, Shanghai Kudos Ultrasonic Instrument Co. Ltd., 59 kHz, 45 W) for 24 h while the reaction temperature was kept at about 25 °C using a recycling water bath. The solid was then collected by filtration, washed with deionized water and ethanol, and dried at room temperature. The solid is insoluble in common organic solvents, but soluble in DMSO. Yield: 75%. Anal. Calc. (%) for $C_{20}H_{30}N_4O_2Sn_2$: C, 40.31; H, 5.07; N, 9.40; and Found (%): C, 39.96; H, 4.94; N, 9.31. Selected FT-IR data, ν(cm^{-1}): ν(OH): 3394(s), ν(NCN): 2080(vs), ν(C=C): 1595(s), ν(C−N): 1313(m), ν(Sn–C): 548, ν(Sn–N): 448. ^{1}H NMR (DMSO-d_6, 400 MHz) δ (ppm): 6.90 (d, J = 8.0 Hz, 4H), 6.64 (d, J = 8.0 Hz, 4H), 0.32 (s, 18H, Hα, ^2J[^{119}Sn–^{1}Hα] = 69 Hz). ^{13}C NMR (DMSO-d_6, 100 MHz) δ (ppm): 135.1 (Ar), 131.2 (Ar), 125.4 (Ar),

113.8 (Ar), 110.2 (NCN), 0.65 (Cα, $^{1}J[^{119}Sn–^{13}C\alpha$ = 520 Hz).^{119}Sn NMR (DMSO-d_6, 400 MHz) δ (ppm): -154.7, TOF-MS: 619 $[M+Na]^{+}$.

2.3.2. Synthesis of [(SnMe$_3$)(4-NO$_2$pcyd)], 2

Complex **2** was prepared in a similar way to **1** with the use of 4-NO_2pcyd (1 mmol, 165 mg) instead of bpH_2, 40 mg (1 mmol) NaOH and 199 mg (1 mmol) trimethyltin chloride. The solid is insoluble in common organic solvents, but soluble in DMSO. Yield: 67%. Anal. Calc. (%) for $C_{10}H_{13}N_3O_2Sn$: C, 36.85; H, 4.02; N, 12.89; and Found (%): C, 36.79; H, 3.91; N, 12.82. Selected FT-IR data, ν (cm^{-1}): ν (NCN): 2036 (vs), ν (C=C): 1602 (s), ν(NO_2): 1592, 1313 (s), ν (C−N): 1129 (m), ν (Sn–C): 541, ν(Sn–N): 451. ^{1}H NMR (DMSO-d_6, 400 MHz) δ (ppm): 6.99 (d, J = 8.0 Hz, 2H), 6.66 (d, J = 8.0 Hz, 2H), 0.54 (s, 9H, Hα, ^{2}J $[^{119}Sn–^{1}H\alpha]$ = 57 Hz). ^{13}C NMR (DMSO-d_6, 100 MHz) δ (ppm): 151.8 (Ar), 132.5 (Ar), 125.8 (Ar), 122.2 (Ar), 119.3 (NCN), -2.41 (Cα, $^{1}J[^{119}Sn–^{13}C\alpha$ = 380 Hz).^{119}Sn NMR (DMSO-d_6, 400 MHz) δ (ppm): 127.9, TOF-MS: 350 $[M+Na]^{+}$.

2.4. DNA-binding studies

The DNA-binding studies were performed in 10 mM Tris–HCl / 10 mM NaCl, buffer solution, pH = 7.2. The DNA stock solution was stored at 4 ˚C in the dark and used within 4 days after preparation. A stock solution of the triorganotin(IV) compounds was prepared by dissolving the complex in an aqueous solution of DMSO as the co-solvent, and then diluted suitably with the corresponding buffer to the required concentrations for all the experiments. The final DMSO concentration never exceeded 0.7% v/v.

Fluorescence quenching experiments were conducted by adding an ethidium bromide solution (3 μM) to the prepared buffer solution of CT-DNA (30 μM) for 2 h, followed by addition to the solution of the respective organotin(IV) compound (in 0.7% DMSO/10 mM Tris-HCl/10 mM NaCl buffer, pH = 7.2) at different concentrations. The samples were excited at 258 nm and emission spectra were recorded at 500-700 nm.

The electronic absorption spectrum of the complex was monitored both in the absence and presence of increasing amounts of CT-DNA in Tris–HCl/NaCl buffer. To confirm the stability of the complexes in the buffered solution at room temperature, a UV–Vis study was performed under conditions similar to those used for the DNA binding studies. The spectral features of the complex exhibited no change in the position of bands and only a very minor change in the intensity over a period of 24 h. No precipitation was observed. This suggests that the complexes are stable under the conditions used. The absorption titration experiment was performed by maintaining the concentration of the metal complex constant at 10 μM while the concentration of DNA was varied over the range 0-8.0 × 10^{-5} M. This was achieved by dissolving appropriate amounts of the metal complex and DNA stock solutions in the buffer while keeping the total volume constant. This resulted in a series of solutions with varying concentrations of DNA but with a constant concentration of the complex. The changes observed in spectral absorbance are larger than any that could be due to experimental error. Baseline corrections were applied in all cases. In order to eliminate the absorbance of DNA itself, reference solutions containing DNA alone were prepared with the same concentration of DNA in each sample. All the UV spectra were recorded after equilibration of the solutions for 10 min at room temperature. The absorption data were analyzed for an evaluation of the intrinsic binding constant, K_b, of the complex with CT-DNA.

CD-spectra of CT-DNA were recorded in the absence and presence of the organotin(IV) compounds at room temperature with a quartz cell of 1 cm path length. Each sample solution was scanned in the range of 220-320 nm, and the CD spectrum was obtained after averaging three scans and subtracting the buffer background.

Viscosity experiments were carried out on an Ubbelohde viscometer, immersed in a thermostatic water-bath maintained at 25 °C. The compounds were added to the DNA solution (C_{DNA} = 3.50 ×10^{-4} M) by microsyringe. Flow time was measured by a digital

stopwatch. The average values of three replicated measurements were used to evaluate the viscosity of the samples. Data were presented as $(\eta/\eta_0)^{1/3}$ versus the ratio of the concentration of compounds to DNA, where η was the viscosity of DNA in the presence of compound and η_0 was the viscosity of DNA alone. Viscosity values were calculated according to the equation $\eta = (t - t_0)/ t_0$, where t was the flow time of the CT-DNA solution in the presence or absence of the complex and t_0 that of the buffer alone.

Cyclic voltammograms of 3.00 mM solutions of each triorganotin(IV) compound in 10% aqueous DMSO with 0.1 M Tetra-n-butyl ammonium perchlorate (TBAP) as supporting electrolyte were obtained in the absence and presence of 50 μM DNA at 25 °C at a scan rate of 100 mV/s. A working electrode (glassy carbon) with a geometric area of 0.071 cm^2 was used. Before the experiments, all solutions were deaerated with dry nitrogen gas for 10 min to remove dissolved oxygen and were kept under a nitrogen atmosphere throughout the experiments.

2.5. Protein binding studies

Absorption titration experiments were performed by keeping the BSA concentration constant (5×10^{-7} M) and varying the concentration of the complex (1.0×10^{-6} M). The samples were equilibrated before recording each measurement for 8 min. Titrations were carried out manually using a micropipette. For recording fluorescence spectra, an excitation wavelength of 280 nm was chosen and very dilute solutions were used in the experiment (BSA 1.0 μM, complexes in the range of 0-14.0 μM) to avoid inner filter effect [37]. The strong fluorescence characteristics of BSA provide a sensitive spectroscopic method to study the interaction with different molecules. The BSA binding experiments with the organotin(IV) compounds (dissolved in 0.7% v/v DMSO) were performed by collecting the fluorescence spectra in 10 mM Tris–HCl, 10 mM NaCl, pH 7.2 buffer solution. To confirm the stability of BSA under the experimental conditions, the UV–Vis spectra of BSA were

recorded in buffer solution alone and then with the same buffer solution containing 0.7% v/v DMSO. As shown in Fig. S1, the absorption spectrum of BSA did not change in the presence of 0.7% v/v DMSO which confirms the stability of BSA in the presence of trace amounts of DMSO. Fluorescence emission spectra were recorded in the wavelength range of 300–400 nm by exciting the BSA at 280 nm, with the excitation and emission slit widths of 5 nm. The fluorescence titrations were carried out by taking a fixed concentration of the BSA solution (1 µM BSA) with increasing amounts of compounds (0-14 µM). The emission spectrum of the BSA solution at 344 nm was recorded and then the various amounts of a stock solution of the complex were added to the BSA solution. After each addition, the solutions were mixed and allowed to stand at the appropriate temperature for 8 min to equilibrate. The fluorescence emission spectra were recorded at room temperature.

2.6. Antioxidant assays

2.6.1. OH• scavenging assay

The hydroxyl radical scavenging activity of the organotin(IV) compounds has been studied in vitro using the Nash method [38]. Hydroxyl radicals were generated by the Fe^{3+}/ascorbic acid system. The detection of hydroxyl radicals was performed by measuring the amount of formaldehyde produced from the oxidation reaction with DMSO. The formaldehyde generated was identified spectrophotometrically at 412 nm. A mixture of 1.0 mL of iron-EDTA solution (0.13% ferrous ammonium sulfate and 0.26% EDTA), 0.5 mL of EDTA solution (0.018%), and 1.0 mL of DMSO (0.85% DMSO (v/v) in 0.1 M phosphate buffer, pH 7.4) were consecutively added to the test tubes. The reaction was initiated by adding 0.5 mL of ascorbic acid (0.22%) and was incubated at 80-90 °C for 15 min in a water bath. After incubation, the reaction was quenched by the addition of 1.0 mL of ice-cold trichloroacetic acid (17.5% w/v). Subsequently, 3.0 mL of Nash reagent was added to each tube and left at

room temperature for 15 min. The intensity of the color formed was determined spectrophotometrically at 412 nm against the reagent blank.

2.6.2. NO• scavenging assay

The assay for nitric oxide scavenging activity is based on a method [39] where sodium nitroprusside in aqueous solution at physiological pH spontaneously produces nitric oxide which interacts with oxygen to generate nitrite ions. These can be estimated using the Greiss reagent. Scavengers of nitric oxide compete with oxygen leading to a lower production of nitrite ions. For the experiment, sodium nitroprusside (10 mM) in phosphate buffered saline was mixed with a fixed concentration of the complex and standards and was incubated at room temperature for 150 min. After the incubation period, 0.5 mL of Griess reagent containing 1% sulfanilamide, 2% H_3PO_4 and 0.1% *N*-(1-naphthyl)ethylenediamine dihydrochloride was added. The absorbance of the chromophore formed was determined at 546 nm.

2.7. In vitro antimicrobial assay

The synthesized compounds were evaluated for their antimicrobial activity by the agar well diffusion method [40]. The bacterial pathogens used in the present study included *Staphylococcus aureus*, *Enterococcus faecalis*, *Escherichia coli* and *Klebsiella pneumonia* and the fungi *Aspergillus niger* and *Candida albicans*. The required nutrient broth and sabouraud dextrose broth were prepared and sterilized at 121 °C. The bacterial strains were inoculated onto nutrient broth (10^8 cells per mL) and fungal strains were inoculated onto sabouraud dextrose broth (10 spores per mL) and incubated overnight. About 30 mL of a sterilized agar medium was transferred aseptically to each sterilized petri plate. The plates were left at room temperature for solidification. The overnight grown bacterial cultures and fungal spores were swabbed onto the solidified media to achieve a lawn of confluent bacterial/fungal growth. A well of 6 mm diameter was made using a sterile cork borer. The

organotin(IV) compounds were added at concentrations of 0 (control), 25, 50, 75 and 100 mg mL^{-1}. Ciprofloxacin and fluconazole were used as positive control drugs for antibacterial and antifungal activities, respectively. The antibacterial assay plates were incubated at 37 °C for 24 h and the antifungal assay plates were incubated at 28 °C for 48 h. After the incubation period, the diameter of the inhibition zone was measured as an indicator for the activity of the compounds. DMSO as solvent never exceeded 1% v/v and controls containing broth media supplemented with only DMSO at the same dilutions used in the experiments were found to be inactive. Each experiment was performed in triplicate.

2.8. In vitro cytotoxic activity

10 mM stock solutions of the studied agents were made up in DMSO and afterwards diluted with nutrient medium to the desired final concentrations (in a range up to 100 mM). A cisplatin stock solution was made in 0.9% NaCl at a concentration of 1.66 mM and then diluted with nutrient medium to the desired final concentrations (in range up to 100 mM). All cells were seeded into a 96-well plate at cell densities of 1000-1500 cells/well, in 100 mL of growth medium and were incubated for 24 h. The final concentration of DMSO per well did not exceed 1%. Cell number/proliferation was measured after 48 h using a standard MTT-based assay [41,42]. Solutions of various concentrations of the examined compounds were added to all wells, except the control wells where only nutrient medium was added. All samples were made up in triplicate.

Cells were incubated for 48 h with the test compounds at 37 °C and 5% CO_2 in a humidified atmosphere. After incubation, 20 mL of MTT solution and 5 mg/mL in phosphate buffer solution (PBS), pH 7.2, was added to each well. Samples were incubated for 4 h at 37 °C with 5% CO_2 in humidified air. Formazan crystals were dissolved in 100 mL of 10% sodium dodecyl sulfate. Absorbance was recorded on an ELISA plate reader (Stat fax2100,

Awareness, USA) after 24 h at a wavelength of 570 nm. The percentage of inhibition was calculated using the ratio between the absorbance of treated and untreated cells.

3. Results and discussion

3.1. Synthesis and characterization

The ligands bpH_2 and 4-NO_2pcyd were synthesized as previously reported [23,26]. The triorganotin(IV) compounds of composition $[(SnMe_3)_2(\mu\text{-}bp)(H_2O)_2]$,(**1**) and $[(SnMe_3)(4\text{-}NO_2pcyd)]$, (**2**) were obtained by sonication of a suspension of $SnMe_3Cl$, and the deprotonated phenylcyanamide ligands with sodium hydroxide (bp^{2-} or 4-NO_2pcyd^-) in EtOH/water (1:1) at room temperature. The compounds are stable in atmospheric conditions and soluble in DMSO.

The infrared data for the ligands, **1** and **2** are listed in Table 1. In the spectrum of **1**, the ν(NCN) band appears at 2080 cm^{-1} compared to 2222 cm^{-1} in the spectrum of free bpH_2. A similar shift of the ν(NCN) band to a lower wavenumber is observed for **2** (2036 cm^{-1} vs 2145 cm^{-1} for free 4-NO_2pcyd) and this suggests coordination of the trimethyltin moiety to the cyano groups of bpH_2 and 4-NO_2pcyd. Furthermore, new bands appear in the 550-538 cm^{-1} and 440-482 cm^{-1} ranges which can be assigned to ν(Sn–C) and ν(Sn–N) vibrations, respectively, thus confirming the formation of the reaction products **1** and **2** [43].

Table 1.

The ^1H NMR spectra of the free ligands and their triorganotin(IV) complexes have been recorded in DMSO. The signals are assigned using their distinct multiplicity patterns, resonance intensities, ^nJ-values and ^{119}Sn satellites (Table 2). The ^1H NMR integration values are consistent with the structures shown in Scheme 1. Representative spectra are given in Figs. S2 and S3. Coordination of ligand bp^{2-} or 4-NO_2pcyd^- to tin causes an up-field shift of the signals of the aromatic protons.

According to the literature, the $^{2}J(^{119}Sn\text{-}^{1}H)$ coupling constants are indicative of the coordination number of trimethyltin(IV) complexes [44-49]. In tetracoordinated tin complexes ^{2}J values should be below 59 Hz; while for pentacoordinated complexes ^{2}J values fall in the 65-80 Hz range [50,51]. The methyl protons in **1** give a characteristic signal at 0.32 ppm with $^{2}J[^{119}Sn–^{1}H]$ = 69 Hz, which falls in the range typical for a five-coordinate trigonal bipyramidal geometry in solution. The methyl protons in **2** give a signal at 0.54 ppm with $^{2}J[^{119}Sn\text{-}^{1}H]$ = 57 Hz, which falls in the range typical for a four-coordinate tetrahedral geometry [52].

Table 2.

^{13}C NMR data and representative spectra are given in Table S1, Figs. S4 and S5. The $^{1}J[^{119}Sn\text{-}^{13}C]$ coupling constants are 520 (**1**) and 380 (**2**) Hz. These values are consistent with those generally observed for five- and four-coordinated tin species, respectively [53,54].

The ^{119}Sn chemical shift values give tentative indications of the environment around the tin atom. The ^{119}Sn chemical shifts do not only depend upon the electron-releasing power of the alkyl and aryl groups but also on the nature of X in R_nSnX_{4-n}. As the electron-releasing power of the alkyl group increases or the electronegativity of X decreases, the tin atom becomes progressively more shielded and the ^{119}Sn resonance moves to higher field [55]. A very important property of the ^{119}Sn chemical shift is that an increase in the coordination number of tin from four to five, six or seven usually produces a large up field shift. According to the literature the δ (^{119}Sn) values of four-coordinate complexes fall in the range +200 to -60 ppm and five-coordinate complexes have chemical shifts between -90 and -190 ppm [56].

The ^{119}Sn NMR spectra of **1** and **2** are given in Figs. S6 and S7. The ^{119}Sn NMR spectra show only a sharp singlet indicating the formation of a single species. The ^{119}Sn resonance of **1** appears at -154.7 ppm and that of **2** at 127.9 ppm suggesting five- and four-coordination, respectively [4].

Mössbauer spectroscopy is another important technique that can be used to provide structural information for organotin compounds [57].The ^{119}Sn Mössbauer spectra of compounds **1** and **2** recorded at 77 K are presented in Fig. 1. The Mössbauer parameters, the quadrupole splitting (Δ) and isomer shift (δ), are listed in Table 3. The coordination number of the tin atom has been related to the ρ value (ratio of Δ/δ). A ρ value less than 1.9 is indicative of tin compounds that are four coordinated while values larger than 2.1 have been assigned to tin complexes with greater than four-coordination [57]. For **1** and **2**, the ρ values are 2.52 and 1.54, respectively. This clearly indicates that compound **2** is four-coordinated, while **1** has a coordination number of five or higher.

Quadrupole splitting values have also been used to distinguish between four and five-coordinated triorganotin structures [58,59]. Quadrupole splitting ranges for regular arrangements of trialkylorganotin(IV) compounds are 1.5–2.8 mm s^{-1} for a tetrahedral geometry, 2.6–3.9 mm s^{-1} for a trigonal bipyramidal geometry and 3.5–4.2 mm s^{-1} for octahedral trans-dialkylorganotin(IV) compounds [60]. **1** and **2** have Δ values of 3.56 mm s^{-1} and 2.10 mm s^{-1}, respectively (Table 3), supporting the assignment of a tetrahedral structure for **2**. The quadrupole-splitting of **1** is consistent with both five- and six-coordination. However, an octahedral geometry has been disregarded since octahedral coordination for triaryl- and trialkylorganotin(IV) compounds is uncommon. Furthermore, the quadrupole splitting of **1** is in agreement with those of trialkylorganotin(IV) carboxylate derivatives with trans-trigonal bipyramidal arrangement (Δ falls in the range 3.0-4.1 mm s^{-1}) [61, 62]. Hence, the Mössbauer results along with the IR, ^{1}H, ^{13}C and ^{119}Sn NMR data give evidence that compound **1** has a five-coordinate metal center generated by cyanamide binding and water coordination.

Fig.1

Table 3.

Fig.2 shows the SEM and TEM images of **1** and **2**. A typical SEM image of **1** is shown in Fig. 2a, which demonstrates that nanowires are formed in large quantities. The nanowires have a width of 10-40 nm and a length of up to tens of micrometers. By careful observation, some of the nanowires have a slight bend and seem to be flexible, probably due to their remarkable long length. Fig. 2b is a representative TEM image, which shows that the nanowires of **1** are straight with a smooth surface and are uniform with an average width of about 30 nm, consistent with the SEM images. The SEM image of compound **2** (Fig. 2c) reveals spherical nanoparticles. The corresponding TEM image (Fig. 2d) confirms that the particle size of these nanoparticles is about 100 nm.

A possible explanation for the nanowire morphology of **1** might be the formation of intermolecular hydrogen bonds between the water ligands that could link the dinuclear complex molecules into a 1D supramolecular structure. This hypothesis is supported by the presence of a broad OH stretching band centered at 3448 cm^{-1} in the FT-IR spectrum of 1 [63].

Fig. 2.

3.2. Stability of the complexes in solution

In order to to identify the species present in solution mass spectra were recorded [Figs. S8 and S9]. When concentrated solutions of the complexes were diluted with a 1:1 water mixture, the mass spectra of showed signals centered at m/z = 619 (**1**) and 350 (**2**) that can be assigned to the isotopomers of $[\mathbf{1}+Na]^+$ and $[\mathbf{2}+Na]^+$. This suggests that the complexes are stable in solution.

3.3. DNA-binding studies

DNA is an important cellular target, many compounds exert their antitumor effects through binding to DNA thereby changing the replication of DNA and inhibiting the growth of the tumor cells, which can be a basis for designing new and more efficient antitumor drugs.

Effectiveness in turn depends on the mode and affinity of the binding [64-67]. Therefore, binding studies of small molecules to DNA are considered to be important tools in the development of DNA molecular probes and new therapeutic reagents [68, 69]. The R_3Sn^+ moieties have been observed to directly affect DNA [70] as well as to bind to membrane proteins or glycoproteins, or to cellular proteins; *e.g.* to ATPase, hexokinase, acetylcholinesterase of human erythrocyte membrane or to skeletal muscle membranes [71]. Furthermore, a wide number of reports have been published concerning the possible mechanisms for the interaction of alkyl or aryltin moieties with the membrane or constituents within the cell [72-75], although the exact mechanism is still unclear. However, it is generally agreed that the R_3Sn^+ fragments may bind to the phosphate groups in DNA [76-78], changing the intracellular metabolism of the phospholipids of the endoplasmic reticulum [79,80].

3.3.1. Viscosity measurements

Non-covalent metal-complex DNA interactions include intercalation, groove binding and electrostatic attraction. Viscosity measurements are usually considered the least ambiguous method to study the DNA binding mode. A classical intercalation model demands that the DNA helix must lengthen as base pairs are separated to take in the binding ligand/complex, leading to an increase of DNA viscosity. In contrast, a partial or non-classical intercalation of the ligand/complex could bend (or kink) the DNA helix, reduce its effective length and concurrently its viscosity [81], while groove binders have no or little effect on the viscosity. The effects of **1** and **2** on the viscosity of CT-DNA at 25 °C were investigated (Fig. S10). The viscosity of CT-DNA decreased with increasing amounts of **1** or **2** with **1** exhibiting the stronger effect. This indicates that **1** interacts more strongly with DNA than **2** (see below) and excludes classical intercalation as the binding mode for both complexes. This is in line with complex **2** having two metal entities on either side of the phenyl ring which should prevent intercalation of the aromatic moiety into the DNA duplex.

3.3.2. Circular dichroism

CD spectroscopy is one of the most common means for monitoring the conformation of DNA in solution. The CD spectrum of DNA exhibits a positive peak at 278 nm due to base stacking and a negative peak at 246 nm due to the helicity of B-type DNA [82, 83]. A simple electrostatic or groove binding interaction of complexes with DNA would show little or no perturbation of the base stacking and helicity bands, while an intercalative interaction would enhance the intensities of both bands [84,85]. The observed CD spectra of CT-DNA in the presence of **1** and **2** show little perturbation of the two bands (Fig. 3), which is indicative of a non-intercalative interaction between the complexes and DNA and thus along with the viscosity data supports a groove binding mode [86, 87].

Fig. 3.

3.3.3. DNA binding study by cyclic voltammetry

The application of cyclic voltammetry to the study of the interaction of metal complexes with DNA provides a useful complementary method [88]. In the present study it has been employed to examine the nature of binding of **1** and **2** to DNA, and the result is shown in Fig. 4. The voltammogram of the complexes **1** and **2** in the absence DNA (Fig. 4(a)) featured a single well defined and stable cathodic peak at -1.473 V and -1.702 V, respectively which reflects the reduction of Sn^{4+} to Sn^{2+}. The absence of an anodic peak in the reverse scan indicated the irreversibility of the electrochemical process. Peak broadening was observed for **1** and **2** which may be attributed to a one step two electron reduction process [89].

In an earlier pioneering study on metal complex–DNA interaction Bard et al. [90] reported a positive shift in peak potential for intercalators that bind *via* hydrophobic interactions (intercalation) and a negative shift of peak potential for electrostatic interactions (groove binding). Upon addition of 50 µM DNA the cathodic peak current dropped by 31.48 (**1**) and 33.69 % (**2**), with negative shifts. For complexes **1** and **2**, the cathodic peaks appeared at -

1.581 and -1.779 V, respectively. This suggests that **1** and **2** may interact with CT-DNA via groove binding in line with the CD and viscosity measurements [91]. Furthermore, the voltammograms of **1** and **2** were collected at different scan rates in the absence and presence of CT-DNA. The peak currents are directly proportional to the square root of the scan rates, indicating that the electrochemical processes of both the free triorganotin compounds and their DNA bound forms are diffusion controlled (Fig. S11) [92]. Moreover, the smaller slope of the plot in the presence of DNA (Fig. S12) demonstrates that the compound-DNA system diffuses more slowly than the free compounds. This finding can be explained by the increase in molecular size and molecular weight after the interaction of the complexs with DNA [93].

Fig.4.

3.3.4. Ethidium bromide-DNA fluorescence quenching

Fluorescence spectral analysis has become a valuable way to determine the binding affinity of metal complexes with DNA [94]. Upon addition of a metal complex the fluorescence of the intercalator ethidium bromide (EB) bound to DNA can be noticeably quenched [95].

The fluorescence spectra of the EB–DNA system quenched by compounds **1** and **2** and the plots of I_0/I vs. r ($C_{[compound]}/C_{[DNA]}$) are shown in Fig. 5. With increasing the concentrations of compounds **1** and **2**, the intensity of the fluorescence spectra emission band at 590 nm of the EB–DNA system is noticeably decreased. The observed linearity in the plot is in good agreement with the linear Stern–Volmer equation [96]:

$$I/I_0 = 1 + K_{sp}r$$

where, I_0 and I are the fluorescence intensities displayed in the absence and presence of the compounds, respectively; r corresponds to the concentration ratio of the compound to DNA. K_{sq}, the linear Stern–Volmer quenching constant, can be obtained from the slope of the I/I_0 versus r linear plot. The calculated values of K_{sq} for compounds **1** and **2** are 4.63 M^{-1} and 2.35 M^{-1} respectively, and indicate stronger interaction between compound **1** and DNA than

449 **2**. From the DNA binding results (Table S2), it is clear that compound **1** presents a higher
450 binding constant (K_b) for DNA when compared to compound **2** which may be due to the
451 existence of the biphenyl unit in the ligand and its polynuclear structure.

452 **Fig. 5.**

453 **3.3.5. UV–vis absorption studies**

454 The DNA binding behavior of the studied organotin(IV) compounds has also been followed
455 through absorption spectral titrations, because absorption spectroscopy is one of the most
456 useful techniques to study the binding of any drug to DNA quantitatively [97-100].
457 Compounds that bind to DNA through intercalation are characterized by a change in
458 absorbance (hypochromism) and a bathochromic shift of the absorption maximum as a result
459 of a strong stacking interaction between the intercalating aromatic chromophore and the DNA
460 base pairs. On intercalation the π* orbital of the intercalator can couple with the π orbital of
461 the DNA bases. As a result the π → π* transition probabilities decrease leading to
462 hypochromism. The extent of hypochromism usually correlates with the strength of the
463 intercalative interaction. A non-intercalative or an electrostatic binding mode with DNA may
464 result in hyperchromism [101].

465 The absorption spectra of compounds **1** and **2** present two well resolved bands at ~263 nm
466 and ~355 nm, which are assigned to intraligand charge transfer (ILCT) transitions and ligand-
467 to-metal charge transfer (LMCT) transitions, respectively. The absorption spectra of
468 compounds **1** and **2** in the absence and presence of CT-DNA are shown in Fig. 6. From the
469 electronic absorption spectral data, it is obvious that on increasing the concentration of DNA
470 added to **1** and **2** both absorption bands display hypochromism accompanied with
471 bathochromic shifts. While UV/vis-spectroscopy is generally not considered an unambiguous
472 method to determine the binding mode, it allows the study of the binding affinity. To

compare the binding strength of the two compounds, the intrinsic binding constant K_b was calculated according to the equation [102]:

$$[DNA] / (\varepsilon_a - \varepsilon_f) = [DNA] / (\varepsilon_b - \varepsilon_f) + 1 / K_b (\varepsilon_b - \varepsilon_f)$$

K_b values of 9.25×10^4 M^{-1} and 3.54×10^4 M^{-1} were obtained for compounds **1** and **2**, respectively. These values are comparable to those reported for other metal complexes (ranging from 10^2 to 10^5 M^{-1}) [101,103]. Compound **1** shows a higher K_b value than **2** in line with the results of the fluorescence quenching studies and viscosity measurements.

In order to compare the DNA binding affinity of **1** and **2** with that of trimethyltin chloride, a UV spectroscopic titration was also carried for this compound (Fig. S13). The addition of CT DNA results in hyperchromism and a K_b value of 5.9×10^3 M^{-1} was obtained for trimethyltin chloride. Thus, the K_b value increases in the order $(CH_3)_3SnCl$ < **1** < **2** and correlates with the more extended aromatic system in **2** compared to **1** which results in stronger interactions with the DNA surface. Furthermore, **2** contains two metal centers that may enhance the binding through additional electrostatic interactions.

Fig.6.

3.4. Protein binding studies

Fluorescence spectroscopy is a useful method for the quantification of the binding of metal complexes to bovine serum albumin (BSA). Generally, the native fluorescence of BSA is caused by three amino acids in the protein, namely tryptophan, tyrosine, and phenylalanine. Environmental alterations around the fluorophore can induce fluorescence quenching which can reveal the nature of the metal complex BSA interaction [104,105]. Fig. 7 shows the effect of increasing the concentration of **1** and **2** on the fluorescence emission of BSA. Addition of compound **1** or **2** to BSA results in the quenching of fluorescence emission intensity due to complex formation between BSA and **1** or **2**. The quenching process can be analyzed by the Stern–Volmer equation [106]:

$$I_0/I = 1 + K_{sv}[Q]$$

where I_0 and I are the fluorescence intensities at 346 nm in the absence and presence of **1** or **2**, respectively. [Q] is the concentration of the quencher and K_{sv} is the Stern–Volmer quenching constant. As shown in Fig. 7, the inset plot of I_0/I versus [Q] exhibits a good linear relationship with linear correlation coefficients of 0.991 and 0.984 for **1** and **2**. The K_{sv} values obtained from the slopes of the linear plots are 1.03×10^5 M^{-1} (**1**) and 1.07×10^5 M^{-1} (**2**). Fluorescence quenching usually occurs by two different mechanisms which are classified as dynamic quenching and static quenching. Dynamic quenching refers to the fluorophore and the quencher coming into contact during the transient existence of the excited state. Static quenching refers to the fluorophore and quencher forming a complex in the ground state. In order to distinguish between these two types of quenching mechanism for BSA/**1** and BSA/**2** UV–Vis absorption spectra were recorded (Fig. S14). The weak absorption peak at about 278 nm in the absence of **1** and **2** displays an increase in intensity, which reveals that fluorescence quenching of BSA by these compounds is mostly a static quenching process [102,107]. For a static quenching interaction, the fluorescence intensity data can also be used to determine the apparent binding constant (K_b) and the number of BSA binding sites (n) for the complex by the following equation [108, 109]:

$$\log ((I_0\text{-}I)/I) = \log K_b + n \log [Q]$$

where K_b is the equilibrium constant and n is the number of binding sites per albumin. n can be calculated from the intercept and slope of the $\log((I_0-I)/I)$ vs log [Q] plot (Fig. S15). K_b values of 1.14×10^5 M^{-1} (**1**) and 2.01×10^6 M^{-1} (**2**) were obtained. n was found to be 1.04 for **1** and 1.25 for **2**, both are close to 1, suggesting that there is only one binding site for these compounds on the BSA molecule. Furthermore, compound **2** showed a higher binding constant with BSA (Table S2), which is similar to the fluorescence emission behaviors of compounds reported earlier [110-112]. It is proposed that compound **2** has a higher binding

affinity for BSA (i.e. quenches the BSA fluorescence more effectively) than compound **1** because of steric reasons. Compound **2** is a mononuclear complex with a para-substituted phenylcyamamide ligand, while compound **1** containing a biphenyl moiety and two $SnMe_3$ entities is more sterically demanding.

Fig.7.

3.5. Antimicrobial activity

The efficiencies of the free ligands, trimethyltin chloride, **1** and **2** have been tested against two Gram-positive bacteria (*Staphylococcus aureus*, *Enterococcus faecalis*), two Gram-negative bacteria (*Escherichia coli*, *Klebsiella pneumonia*) and fungal strains (*Aspergillus niger* and *Candida albicans*) by an agar well diffusion method. The effectiveness of an antimicrobial agent in sensitivity testing is based on the size of the diameter zones of inhibition against Gram-positive, Gram negative bacteria and fungal strains. The diameter of the zone is measured to the nearest millimeter and the data are given in Table 4 and the minimum inhibitory concentration is displayed in Table S3. Inhibition zones were measured and compared with the current antimicrobial drugs ciprofloxacin (antibacterial) and fluconazole (antifungal). A comparison of the antimicrobial activities of **1** and **2** with the free ligands shows that the triorganotin(IV) complexes are more toxic than their parent ligands against the same microorganisms under identical experimental conditions. However, they are better antibacterial agents than antifungal agents. Furthermore, the antimicrobial activity values for complexes **1** and **2** are higher than those for trimethyltin chloride except for *A. niger* for which the trimethyltin chloride shows strong activity. Moreover, compound **1** was found to have higher activity against the different strains of bacteria and fungi than complex **2**. Also, compound **1** exhibited an almost equipotent activity (zone of inhibition = 29 mm) with the standard drug ciprofoxacin (zone of inhibition = 32 mm) against *Enterococcus faecalis.* Compounds **1** and **2** exhibited good activity against all the other bacteria tested with

548 inhibition zones of 15–29 mm. Compound **1** (17 mm) and **2** (21 mm) exhibited comparable
549 antibacterial activities toward *K. pneumoniae*.

550 Thus, the evaluation of the in vitro antifungal activity showed that the free ligands were
551 almost inactive while **1** and **2** displayed a moderate activity. Compounds **1** and **2** were found
552 to be less active against the yeast *C. albicans*, but moderate antifungal activity was exhibited
553 by both compounds against the pathogenic mould *A. niger*.

554 **Table 4.**

555 **3.6. Evaluation of radical scavenging ability**

556 The radical scavenging activities of the free ligands, trimethyltin chloride, **1** and **2** along
557 with standard reference compounds, such as butylated hydroxyl toluene (BHT) and Vitamin
558 C in a cell free system, have been studied with reference to hydroxyl radicals (OH•) and nitric
559 oxide (NO•). The corresponding IC_{50} values are shown in Table S4. From Table S4, it can be
560 deduced that the free ligands and trimethyltin chloride have a significantly lower scavenging
561 activity than **1** and **2**. **1** showed better activity than **2**. On the whole, the scavenging activity
562 was found to increase in the order of Vitamin C < BHT < $(CH_3)_3SnCl$ < 4-NO_2pcyd < bpH_2 <
563 **2** < **1** (Fig. S16). The IC_{50} values (Table S4) indicate that all compounds are better OH•
564 scavengers than NO• scavengers. The lower IC_{50} values observed in the antioxidant assays
565 suggest that these compounds have a strong potential to act as scavengers for the elimination
566 of radicals. Also, it is worthy of note that **1** and **2** possess superior antioxidant activity against
567 the above mentioned radicals than do the standard antioxidants butylated hydroxyl toluene
568 (BHT) and vitamin C.

569 **3.7. In vitro cytotoxicity studies**

570 The positive results obtained from the above biological studies namely, DNA binding,
571 BSA binding, antioxidative studies and antimicrobial activity of complexes **1** and **2** prompted
572 us to test their cytotoxicity against a panel of human tumor cell lines including A549, Du145,

HeLa and MCF-7 using the MTT assay [113]. Cells were treated for 48 h with **1** and **2** and with cisplatin as a positive control. Untreated cells were used as a negative control. Both compounds showed a dose-dependent growth inhibitory effect against the tested cell lines (Fig. 8). Compound **1** exhibits a promising growth inhibitory effect against HeLa cells that is slightly higher than that observed for cisplatin (Table 5). Our current results are in agreement with previous literature reports that showed that organotin(IV) - and particularly triorganotin compounds - exhibit antiproliferative effects in various cancer cell lines [114, 115]. Triphenyltin(IV) complexes, for example, are known to have higher antiproliferative effects compared to diorganotin(IV) derivatives against different cell lines [116-119]. The IC_{50} values of the triorganotin(IV) compounds **1** and **2** indicate a potent cytotoxic effect at micromolar concentration which warrants further mechanistic investigation. Trimethyltin chloride and the free ligands bpH_2 and 4-NO_2pcyd after 48 h of incubation exhibited very low cytotoxic activity and did not reach IC_{50} values in the applied concentration range (up to 100 μM) in all investigated cell lines.

Fig. 8

Table 5.

4. Conclusions

In summary, triorganotin(IV) complexes of formula [$(SnMe_3)_2$(μ-bp)$(H_2O)_2$], **1**, and [$(SnMe_3)$(4-NO_2pcyd)], **2**, (Me: methyl, bpH_2: 4,4′-dicyanamidobiphenyl and 4-NO_2pcyd: 4-nitrophenylcyanamide) have been synthesized *via* a sonochemical process. The molecular structures of the triorganotin(IV) complexes were determined by FT-IR, multinuclear NMR (^{1}H, ^{13}C and ^{119}Sn), Mössbauer spectroscopy, elemental analysis, SEM and TEM. The DNA binding properties of the two complexes were explored by electronic absorption, fluorescence spectroscopy, CD spectra, CV and viscosity measurements. The results suggested that both complexes could interact with CT-DNA *via* the groove binding mode and they follow the

binding affinity order of **2** < **1**. The reactivity towards BSA revealed that complex **2** exhibits greater binding affinity than that of complex **1**. Compound **1** shows stronger antimicrobial activity than **2**, but both are more reactive against Gram-positive bacteria than against Gram-negative bacteria and fungi. Also, complexes **1** and **2** have more antioxidant activity than the free ligands, trimethyltin chloride, butylated hydroxyl toluene (BHT) and vitamin C. The cytotoxicity studies show that the complexes exhibit high cytotoxic activity against different cell lines tested. Also, the results of cytotoxicity revealed that the metal complexes are more effective than their respective free ligands and trimethyltin chloride under identical experimental conditions.

Acknowledgement

We are grateful for the financial support from the Department of Chemistry, Isfahan University of Technology (IUT).

References

[1] W. Jiang, E. Papa, H. Fischer, S. Mardyani, W. C. W. Chan, Trends Biotechnol. 22 (2004) 607.

[2] J. L. Sessler, S. R. Doctrow, J. McMurry, S. J. Lippard (Eds.), Medicinal Inorganic Chemistry, American Chemical Society, Washington, DC, 2005.

[3] Q. S. Li, M. F. C. Guedes da Silva, A. J. L. Pombeiro, Chem. Eur. J. 10 (2004) 1456.

[4] M. Hong, H. Geng, M. Niu, F. Wang, D. Li, J. Liu, H.Yin, Eur. J. Med. Chem. 86 (2014) 550.

[5] X. M. Shang, J. Z. Wu, A. J. L. Pombeiro, Q. S. Li, Appl. Organomet. Chem. 21 (2007) 919.

[6] Q. S. Li, M. F. C. Guedes da Silva, J. H. Zhao, A. J. L. Pombeiro, J. Organomet. Chem. 689 (2004) 4584.

622 [7] X. M. Shang, J. Z. Wu, A. J. L. Pombeiro, Q. S. Li, J. Inorg. Biochem. 102 (2008)
623 901.
624 [8] P. G. Harrison, Chemistry of Tin. Chapman &Hall, London, 1989.
625 [9] I. Omae, Organotin Chemistry.J. Organomet. Chem. Library 21. Elsevier Science
626 Publishers B. V., New York, 1989.
627 [10] M. Gielen, Tin-based Antitumor drugs. Springer-Verlag, Berlin, 1990.
628 [11] A. J. Crowe, P. J. Smith and G. Atassi, Inorg.Chim. Acta 93 (1984) 179.
629 [12] M. Gielen, Main Group Met. Chem. 17 (1994) 1.
630 [13] M. Gielen, R. Willem, J.Holecek and A. Licka, Main Group Met. Chem. 16 (1993)
631 29.
632 [14] J. J. Zuckerrnann (Ed.), Organotin Compounds: New Chemistry and Applications,
633 Adv.Chem. Ser. 157. American Chemical Society, Washington, D.C., 1976.
634 [15] N. F. Cardarelli (Ed.), Tin as a Vital Nutrient: Implications in Cancer Prophylaxis and
635 other Physiological Processes. CRC Press, Boca Raton, Florida, 1986.
636 [16] A. Sylph, Bibliography on the Effects of Organotin Compounds on Aquatic
637 Organisms, Bibliogr. II. International Tin Research Council, Greenford, U.K., 1987.
638 [17] H. M. Badawi, W. Forner, J. Mol. Struct. (THEOCHEM) 673 (2004) 223.
639 [18] M. Khorasani-Motlagh, M. Noroozifar, S. Niroomand, B. O. Patrick, Inorg. Chim.
640 Acta 383 (2012) 72.
641 [19] R. J. Crutchley, Coord. Chem. Rev. 219 (2001)125.
642 [20] A. Escuer, F. A. Mautner, N. Sanz, R. Vicente, Polyhedron 23 (2004) 1409.
643 [21] M. A. Fabre, J. Jaud, J. Bonvoision, Inorg. Chim. Acta 358 (2005) 2384.
644 [22] H. Chiniforoshan, N. Safari, J. Mohammadnezhad, H. Hadadzadeh, A. H.
645 Mahmoudkhani, Inorg. Chim. Acta 359 (2006) 2101.

[23] H. Chiniforoshan , N. Pourrahim , L.Tabrizi , H. Tavakol , M. R. Sabzalian, B. Notash, Inorg. Chim. Acta 416 (2014) 85.

[24] H. Chiniforoshan, L. Tabrizi, N. Pourrahim, Appl.Electrochem. 45 (2015) 197.

[25] H. Chiniforoshan , S. BahmanpourKhalesi, L.Tabrizi, A. R. Hajipour, A. NajafiChermahini and M. Karimzadeh, J. Mol. Struct. 1082 (2015) 56.

[26] L. Tabrizi, H. Chiniforoshan, Dalton Trans. 44 (2015) 2488.

[27] R. J. Crutchley, M. L. Nakicki, Inorg. Chem. 28 (1989) 1955.

[28] R. J. Crutchley, R. Hynes, E. Gabe, Inorg. Chem. 29 (1990) 4921.

[29] W. Zhang, C. Bensimon, R. J. Crutchley, Inorg. Chem. 32 (1993) 5808.

[30] A. R. Rezvani, R. J. Crutchley, Inorg. Chem. 33 (1994) 170.

[31] W. B. Connick, R. E. Marsh, W. P. Schaefer, H. B. Gray, Inorg. Chem. 36 (1997) 913.

[32] G. Arena, G. Calogera, S. Campagna, L. Scolaro, V. Ricevuto, R. Romaeo, Inorg. Chem. 37 (1998) 2763.

[33] H. Hadadzadeh, A. R. Rezvani and F. Belanger-Gariepy, J. Mol. Struct. 740 (2005) 165.

[34] D. T. Mapolelo, M. Al-Noaimi, R. J. Crutchley, Inorg. Chim. Acta 359 (2006) 1458.

[35] A. S. de Oliveira, L. C. Lianes, R. J. Nunes, R. A. Yunes, I. M. C. Brighente, Green and Sustainable Chemistry, 4 (2014) 177.

[36] J. T. Li, M. X. Sun, Y. Yin, Ultrasonics Sonochemistry, 17 (2010) 359.

[37] Q. Xiao, S. Huang, Y. Liu, F.-f. Tian, J.-c. Zhu, J. Fluoresc. 19 (2009)317.

[38] T. Nash, Biochem. J. 55 (1953) 416.

[39] L. C. Green, D. A. Wagner, J. Glogowski, P. L. Skipper, J. S. Wishnok, S. R. Tannenbaum, Anal. Biochem. 126 (1982) 131.

[40] C. Perez, M. Pauli, P. Bazerque, Acta Biol. Med. Exp. 15 (1990) 113.

671 [41] H. D. Yin, C. H. Yue, M. Hong, J. C. Cui, Q. K. Wu, X. Y. Zhang, Eur. J. Med.
672 Chem. 58 (2012) 533.
673 [42] M. Hong, H. D. Yin, X. Y. Zhang, C. Li, C. H. Yue, S. Cheng, J. Organomet.Chem.,
674 724 (2013) 23.
675 [43] M. Nath, S. Pokharia, R. Yadav, Coord. Chem. Rev. 95 (2001) 215.
676 [44] M. Gielen, R. Willem, B. Wrackmeyer, Advanced Applications of NMR to
677 Organometallic Chemistry; John Wiley and Sons, Ltd.: Chichester, U.K., 1996
678 [45] T. P. Lockhart, W. F. Manders, J. J. Zuckerman, J. Am. Chem. Soc. 107 (1985) 4546.
679 [46] J. Holecek, A. Lycka, Inorg. Chim. Acta 118 (1986) L15.
680 [47] J. P. Quintard, M. Degueil-Castaing, G. Dumartin, B. Barbe, M. Petraud, J.
681 Organomet. Chem. 234 (1982) 234.
682 [48] F. Ahmad, S. Ali, M. Parvez, A. Munir, M. Mazhar, K. M. Khan, T. Ali Shah,
683 Heteroatom Chemistry, 13 (2002) 638.
684 [49] S. Rehman, S. Ali, A. Badshah, A. Malik, E. Ahmed, G.-X. Jin, E. R. T. Tiekink,
685 Appl. Organometal. Chem. 18 (2004) 401.
686 [50] J. Holecek, M. Nadvornik, K. Handlir, A. Lycka, J. Organomet. Chem. 315 (1986)
687 299.
688 [51] T. P. Lockhart, W. F. Manders, Inorg. Chem. 25 (1986) 892.
689 [52] Y. Farina, A. Graisa, E. Yousif, Model. Appl. Sci. 3 (2009) 215.
690 [53] T. P. Lockhart, W. F. Manders, E. M. Holts, J. Am. Chem. Soc. 108 (1986) 6611.
691 [54] W. F. Howard, R. W. Crecely, W. H. Nelson, Inorg. Chem. 24 (1985) 2204.
692 [55] J. Holecek, A. Lycka, K. Handlir, M. Nadvornik, Collect. Czech. Chem. Commun. 55
693 (1990) 1193.
694 [56] J. Holecek, M. Nadvornik, K. Handlir, A. Lycka, J. Organomet. Chem. 315 (1986)
695 299.

[57] R. H. Herber, H. A. Stöckler, W. T. Reichle, J. Chem. Phys. 42 (1965) 2447.

[58] X. Song, C. Cahill, G. Eng, Main Group Metal Chem. 25 (2002) 177.

[59] X. Song, C. Cahill and G. Eng, Main Group Metal Chem. 25 (2002) 703.

[60] R.V. Parish, in: G.J. Long (Ed.), Mossbauer Spectroscopy Applied to Inorganic Chemistry, Plenum Press, New York, 1984.

[61] T. S. B. Baul, S. Dhar, S. M. Pyke, E. R. T. Tiekink, E. Rivarola, R. Butcher, F.E. Smith, J. Organomet. Chem. 633 (2001) 7.

[62] R. Willem, I. Verbruggen, M. Gielen, M. Biesemans, B. Mahieu, T. S. B. Baul, E. R. T. Tiekink, Organometallics 17 (1998) 5758.

[63] J. Luo, T. Lei, L.Wang, Y. Ma, Y. Cao, J. Wang, J. Pei, J. Am. Chem. Soc. 131 (2009) 2076.

[64] A.E. Friedman, C.V. Kumar, N.J. Turro, J.K. Barton, Nucleic Acids Res. 19 (1991) 2595.

[65] A.M. Pyle, T. Morri, J.K. Barton, J. Am. Chem. Soc. 112 (1990) 9432.

[66] J.K. Barton, J.M. Goldberg, C.V. Kumar, N.J. Turro, J. Am. Chem. Soc. 108 (1986) 2081.

[67] P.H. Proctor, E.S. Reynolds, Physiol. Chem. Phys. Med. NMR. 16 (1984) 175.

[68] K.E. Erkkila, D.T. Odom, J.K. Barton, Chem. Rev. 99 (1999) 2777.

[69] B.N. Trawick, A.T. Danihe, J.K. Bashkin, Chem. Rev. 98 (1998) 939.

[70] M.L. Falcioni, M. Pellei, R. Gabbianelli, Mutat. Res. 653 (2008) 57.

[71] L. Pellerito, L.Nagy, Coord. Chem. Rev. 224 (2002) 111.

717 [72] C. Syng-Ai, T.S. Basu Baul, A. Chatterijee, J. Environ. Pathol. Toxicol. Oncol. 20
718 (2001) 333.
719 [73] F. Barbieri, M. Viale, F. Sparatore, G. Schettini, A. Favre, C. Bruzzo, F. Novelli,
720 A. Alema, Anticancer Drug 13 (2002) 599.
721 [74] H. Seibert, S. Moerchel, M. Guelden, Cell. Biol. Toxicol. 20 (2004) 273.
722 [75] N. Hoti, J. Ma, S. Tabassum, Y. Wang, M. Wu, J. Biochem. 134 (2003) 521.
723 [76] Q. Li, N. Jin, P. Yang, J. Wan, W. Wu, J. Wan, Synt. React. Inorg. Met.-Org. Chem.
724 27 (1997) 811.
725 [77] Q. Li, P. Yang, H. Wang, M. Guo, J. Inorg. Biochem. 64 (1996) 181.
726 [78] J.S. Casas, E.E. Castellano, M.D. Couce, J. Ellena, A. Sanchez, J.L. Sanchez, J.
727 Sordo, C. Taboada, Inorg. Chem. 43 (2004) 1957.
728 [79] Y. Arakawa, Biomed. Res. Trace Elem. 4 (1993) 129.
729 [80] Y. Arakawa, Biomed. Res. Trace Elem. 11 (2000) 259.
730 [81] I. H. Bhat, S. Tabassum, Spectrochim. Acta Part A: Mol. Biomol. Spectrosc. 72
731 (2009) 1026.
732 [82] H. Y. Liu, L. Z. Li, Q. Guo, J. F. Dong, J. H. Li, Transit. Met. Chem. 38 (2013)
733 441.
734 [83] P. Li, M. J. Niu, M. Hong, S. Cheng, J. M. Dou, J. Inorg. Biochem. 137 (2014) 101.
735 [84] N. Shahabadi, S. Kashanian, F. Darabi, DNA Cell Biol. 28 (2009) 589.
736 [85] N. Shahabadi, F. Darabi, M. Maghsudi, S. Kashanian, DNA Cell Biol. 29 (2010) 329.
737 [86] P.U. Maheswari, M. Palaniandavar, J. Inorg. Biochem. 98 (2004) 219.

[87] Z. Zhang, X.H. Qian, Int. J. Biol. Macromol. 38 (2006) 59.

[88] S. Mahadevan, M. Palaniandavar, Inorg. Chem. 37 (1998) 693.

[89] S. Shujha, A. Shah, Z..Rehman, N. Muhammad, S. Ali, R. Qureshi, N. Khalid, A. Meetsma, Eur. J. Med. Chem. 45 (2010) 2902.

[90] M. T. Carter, M. Rodriguez, A. J. Bard, J. Am. Chem. Soc. 111 (1989) 8901.

[91] T. S. Pitchumony, P. Mallayan, Inorg. Chim. Acta 337 (2002) 420.

[92] A. J. Bard, L. R. Faulkner, in Electrochemical Methods: Fundamentals and Applications, Wiley, New York, 1980.

[93] Q. X. Wang, F. Gao, K. Jiao, Electroanalysis 20 (2008) 2096.

[94] J. F. Dong, L. Z. Li, D. Q. Wang, Chin. J. Chem. 29 (2011) 259.

[95] H. D. Yin, H. Liu, M. Hong, J. Organomet. Chem. 713 (2012) 11.

[96] J. R. Lakowicz, G. Weber, Biochemistry 12 (1973) 4161.

[97] T.M. Kelly, A.B. Tossi, D.J. McConnell, T.C. Strekas, Nucleic Acids Res. 13 (1985) 6017.

[98] J.K. Barton, A.T. Danishefsky, J.M. Goldberg, J. Am. Chem. Soc. 106 (1984) 2172.

[99] S.A. Tysoe, R.J. Morgan, A.D. Baker, T.C. Strekas, J. Phys. Chem. 97 (1993) 1707.

[100] R.F. Pasternack, E.J. Gibbs, J.J. Villafranca, Biochemistry 22 (1983) 2406.

[101] R. S. Kumar, S. Arunachalam, V. S. Periasamy, C. P. Preethy, A. Riyasdeen, M. A. Akbarsha, J. Inorg. Biochem. 103 (2009) 117.

[102] P. Krishnamoorthy, P. Sathyadevi, R. R. Butorac, A. H. Cowley, N. S. P. Bhuvaneshc, N. Dharmaraj, Dalt. Trans. 41 (2012) 4423.

[103] P. P. Silva, W. Guerra, J. N. Silveira, A. M. C. Ferreira, T. Bortolotto, F. L. Fischer, H. Terenzi, A. Neves, E. C. Pereira-Maia, Inorg. Chem. 50 (2011) 6414.

761 [104] W. S. VanScyoc, B. R. Sorensen, E. Rusinova, W. R. Laws, J. B. A. Ross, Biophys.
762 J. 83 (2002) 2767.
763 [105] L. Z. Li, Q. Guo, J. F. Dong, T. Xu, J. H. Li, J. Photochem. Photobiol. B 12 (2013)
764 556.
765 [106] C. X. Wang, F. F. Yan, Y. X. Zhang, L. Ye, J. Photochem. Photobiol. A Chem. 192
766 (2007) 23.
767 [107] P. Sathyadevi, P. Krishnamoorthy, R. R. Butorac, A. H. Cowley, N. S. P. Bhuvanesh
768 and N. Dharmaraj, Dalton Trans. 40 (2011) 9690.
769 [108] B. Ahmad, S. Parveen, R. H. Khan, Biomacromolecules 7 (2006) 1350.
770 [109] Y. J. Hu, Y. Liu, J. B. Wang, X. H. Xiao and S. S. Qu, J. Pharm. Biomed. Anal., 36
771 (2004) 915.
772 [110] A. K. Singh, A. Asefa, Luminescence 24 (2009)123.
773 [111] R. Hurley, A. C. Testa, J. Am. Chem. Soc. 90 (1968) 1949.
774 [112] S. Undenfriend, Fluorescence Assay in Biology and Medicine, New York: Academic
775 Press, 1962.
776 [113] T. Mosmann, J. Immunol. Methods 65 (1983) 55.
777 [114] S. Gomez-Ruiz, G. N. Kaluderovic, S. Prashar, E. Hey-Hawkins, A. Eric, Z. Zizak,
778 Z. D. Juranic, J. Inorg. Biochem. 102 (2008) 2087.
779 [115] S. K. Hadjikakou, I. I. Ozturk, M. N. Xanthopoulou, P. C. Zachariadis, S. Zartilas,
780 S. Karkabounas, N. Hadjiliadis, J. Inorg. Biochem. 102 (2008) 1007.
781 [116] I. C. Mendes, J. P. Moreira, J. D. Ardisson, R. G. Santos, P. R. da Silva, I. Garcia,
782 A. Casti-neiras, H. Beraldo, Eur. J. Med. Chem. 43 (2008) 1454.
783 [117] M. Gielen, K. Handlir, M. Hollein, D. de Vos, Met. Based Drugs 7 (2000) 233.
784 [118] M. Gielen, M. Biesemans, D. de Vos, R. Willem, J. Inorg. Biochem. 79 (2000)139.

[119] M. N. Xanthopoulou, S. K. Hadjikakou, N. Hadjiliadis, M. Schurmann, K. Jurkschat, A. Michaelides, S. Skoulika, T. Bakas, J. Binolis, S. Karkabounas, K. Charalabopoulos, J. Inorg. Biochem. 96 (2003) 425.

Figure legends

Fig. 1. ^{119}Sn Mössbauer spectra of compounds **1** and **2** at 77 K.

Fig. 2. SEM images of compounds **1** (a) and **2.** (c) TEM images of compounds **1** (b) and **2** (d).

Fig.3. CD-spectra of CT-DNA in the absence and presence of the compound, [DNA]= 1.0×10^{-4} M, [compound] = 0 and 4.0×10^{-5} M.

Fig. 4. Cyclic voltammograms of 3 mM **1** and **2** in the absence (a) and presence (b) of 50 μM CT-DNA in buffer (scan rate = 100 mV/s).

Fig.5. Effects of compounds **1** and **2** on the fluorescence spectrum of the EB–DNA system (λ_{ex} = 258 nm); C_{DNA} = 30 μM; C_{EB} = 3μM; from 1 to 8 $C_{compound}$ = 0, 3, 9, 15, 30, 60, 90, 120 μM, respectively. Arrow shows changes in the emission intensity upon addition of increasing concentration of the compound. Inset: plot of I_0/I vs r ($r = C_{compound}/C_{DNA}$) for compounds **1** and **2**.

Fig. 6. UV–vis absorption spectrum of compounds **1** and **2** (1.0×10^{-5} M) in the absence and presence of CT-DNA, from 1 to 6, [DNA] = 0, 2.0×10^{-5}, 4.0×10^{-5}, 6.0×10^{-5}, $8 \times 10^{-5}$and 10×10^{-5} M, respectively. Arrows show the changes in absorbance with respect to an increase in the DNA concentration (Inset: plot between [DNA] and [DNA] / [$\varepsilon_a - \varepsilon_f$]).

Fig. 7. Fluorescence emission spectra of BSA in the absence and presence of compounds **1** or **2**. [BSA] = 1.0×10^{-6} M, [Compound] = 0, 2.0×10^{-6} M, 4.0×10^{-6} M, 6.0×10^{-6} M, 8.0×10^{-6} M, 10.0×10^{-6} M, 12.0×10^{-6} M, 14.0×10^{-6} M, respectively; λ_{ex} =280 nm, both excitation and emission slits were 5 nm. (Inset: Plot of [Q] vs. I_0/I).

Fig. 8. In-vitro cytotoxicity of compounds **1** and **2** against HeLa tumor cells. Cytotoxicity was measured by the MTT reduction assay after 48 h. Untreated cells are used as the control.

Table1. Infrared spectra of the ligands and triorganotin compounds **1** and **2**.

Vibration	bpH_2	**1**	$4\text{-}NO_2pcyd$	**2**
ν(NCN)	2222	2080	2145	2036
ν(C=C)	1617	1595	1611	1602
$\nu(NO_2)$	-	-	1597, 1337	1592, 1313
ν(Sn-C)	-	548	-	541
ν(Sn-N)	-	448	-	451

Table2. ^{1}H-NMR of free ligands and compounds **1**, **2**.

Observed protons	bpH_2	4-NO_2pcyd	**1**	**2**
Phenyl	7.05 (d, 4H)	7.06 (d, 2H)	6.90 (d, 4H)	6.99 (d, 2H)
	7.62 (d, 4H)	7.92 (d, 2H)	6.64 (d, 4H)	6.66 (d, 2H)
Amine	10.23 (s, 2H)	9.88 (d, 2H)	-	-
Sn-CH_3 (Hα)	-	-	0.32 (s, 18H)	0.54 (s, 9H)
^{2}J [^{119}Sn–^{1}Hα] (Hz)	-	-	69	57

Table3. Mössbauer parameters collected at 77 K of the organotin(IV) derivatives

Product	δ (mm s^{-1})	Δ (mm s^{-1})	ρ
1	1.41	3.56	2.52
2	1.36	2.10	1.54

Table 4. Antibacterial and antifungal activity of the free ligands and compounds **1** and **2**– zone of inhibition in mm

Compounds	Gram-positive		Gram-negative		Fungi	
	S. aureus[a]	*E. faecalis*[b]	*E. coli*[c]	*K. pneumoniae*[d]	*A. niger*[e]	*C. albicans*[f]
bpH_2	08	07	05	10	05	06
4-NO_2pcyd	05	09	07	11	04	03
$(CH_3)_3SnCl$	15	14	13	12	18	07
1	24	29	19	21	15	12
2	19	23	15	17	10	09
Ciprofloxacin	29	32	30	34	—	—
Fluconazole	—	—	—	—	24	32
Control	—	—	—	—	—	—

[a] *Staphylococcus aureus*. [b] *Enterococcus faecalis*. [c] *Escherichia coli*. [d] *Klebsiella pneumonia*. [e] *Aspergillusniger*. [f] *Candida albicans*. "—" no activity.

Table 5. IC_{50} (μM) values of the compounds **1**, **2** and cisplatin against selected cell lines.

compound	A549	Du145	HeLa	MCF-7
bpH_2	> 100	> 100	> 100	> 100
4-NO_2pcyd	> 100	> 100	> 100	> 100
$(CH_3)_3SnCl$	> 100	> 100	> 100	> 100
1	16± 1.3	22± 0.9	17± 0.9	35± 1.2
2	45 ± 1.2	25± 1.7	35 ± 0.8	42± 1.2
Cisplatin	12 ± 1.0	6 ± 1.5	19 ± 1.2	21 ± 1.2

IC_{50} values are given in μM, cisplatin is included for comparison. Data are presented as mean values ± standard deviations and cell viability assessed after 48 h of incubation.

The sign (>) indicates that IC_{50} value is not reached in the examined range of concentrations (the sign is in front of the maximum value of the concentration in the examined range of concentrations).

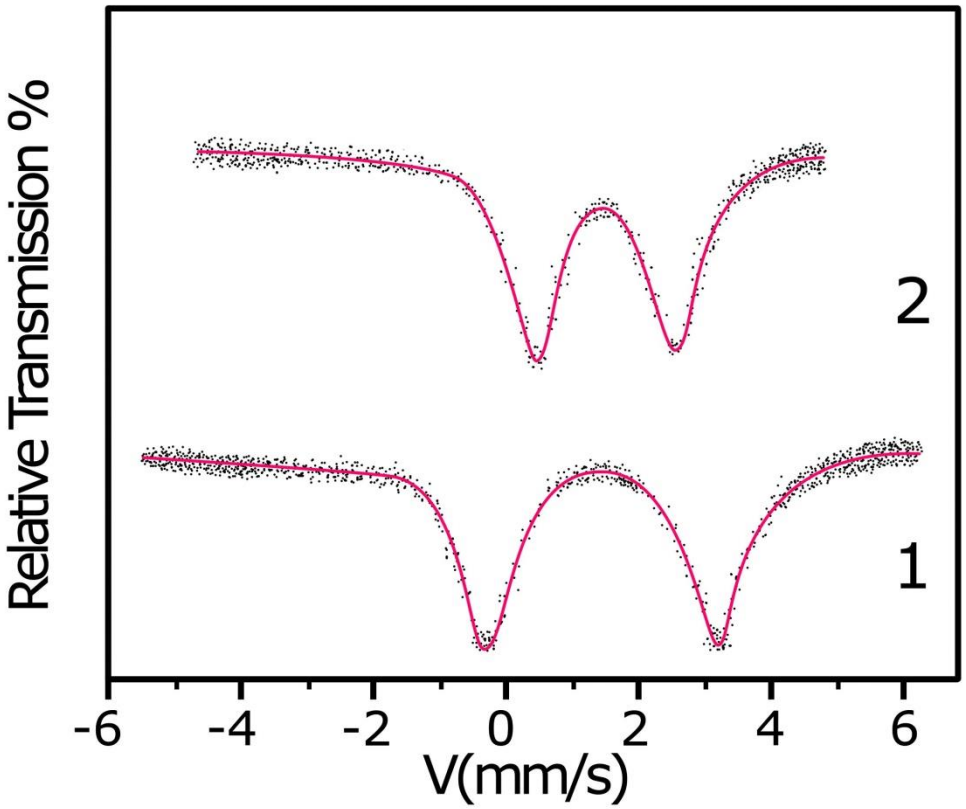

Fig. 1. ^{119}Sn Mössbauer spectra of compounds **1** and **2** at 77 K.

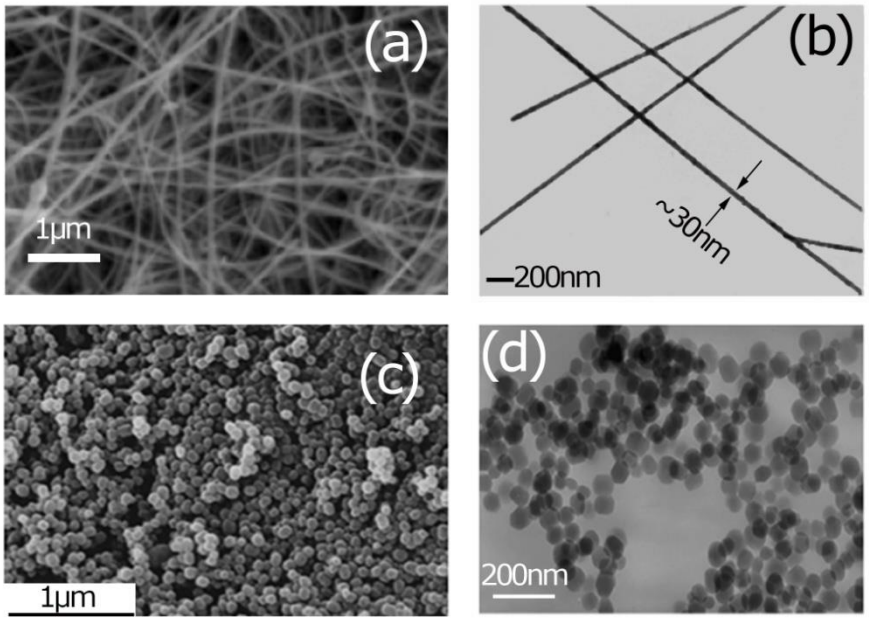

Fig. 2. SEM images of compounds **1** (a) and **2.** (c) TEM images of compounds **1** (b) and **2** (d).

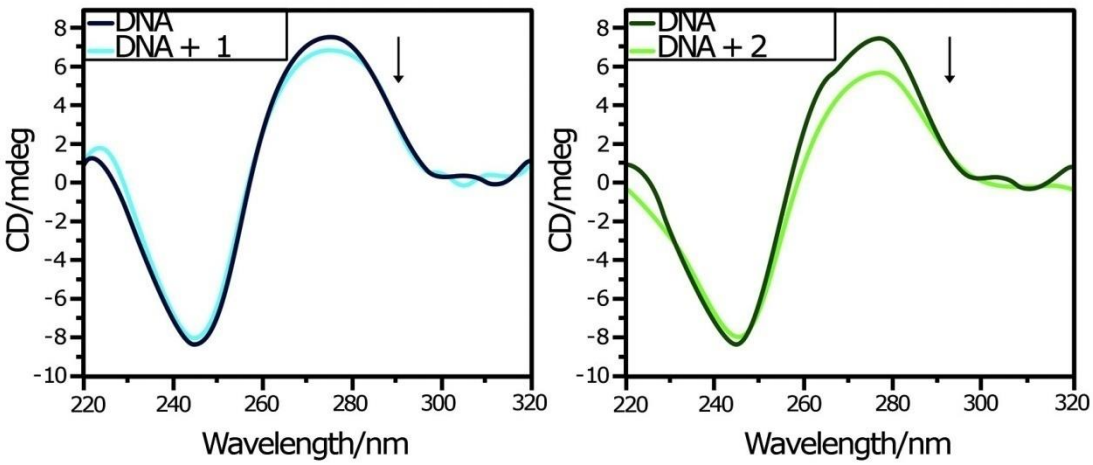

Fig.3. CD-spectra of CT-DNA in the absence and presence of the compound, [DNA]= 1.0×10^{-4} M, [compound] = 0 and 4.0×10^{-5} M.

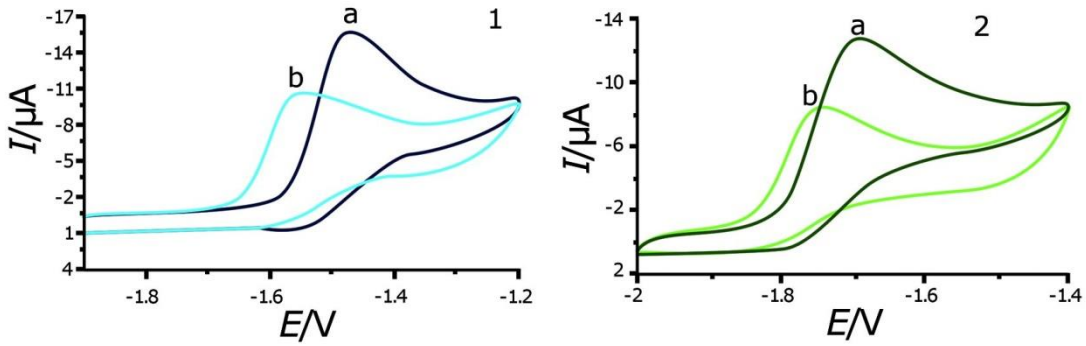

Fig. 4. Cyclic voltammograms of 3 mM **1** and **2** in the absence (a) and presence (b) of 50 μM CT-DNA in buffer (scan rate = 100 mV/s).

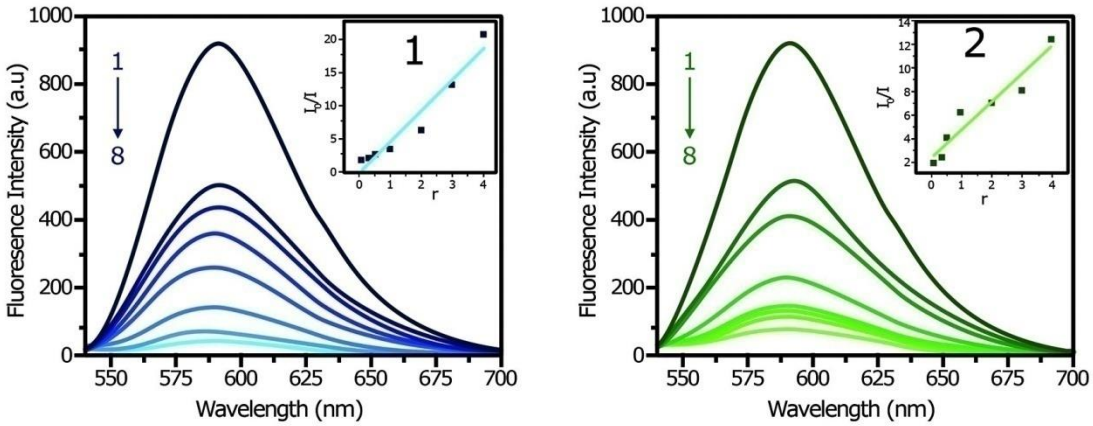

Fig.5. Effects of compounds **1** and **2** on the fluorescence spectrum of the EB–DNA system (λ_{ex} = 258 nm); C_{DNA} = 30 μM; C_{EB} = 3μM; from 1 to 8 $C_{compound}$ = 0, 3, 9, 15, 30, 60, 90, 120 μM, respectively. Arrow shows changes in the emission intensity upon addition of increasing concentration of the compound. Inset: plot of I_0/I vs r ($r = C_{compound}/C_{DNA}$) for compounds **1** and **2**.

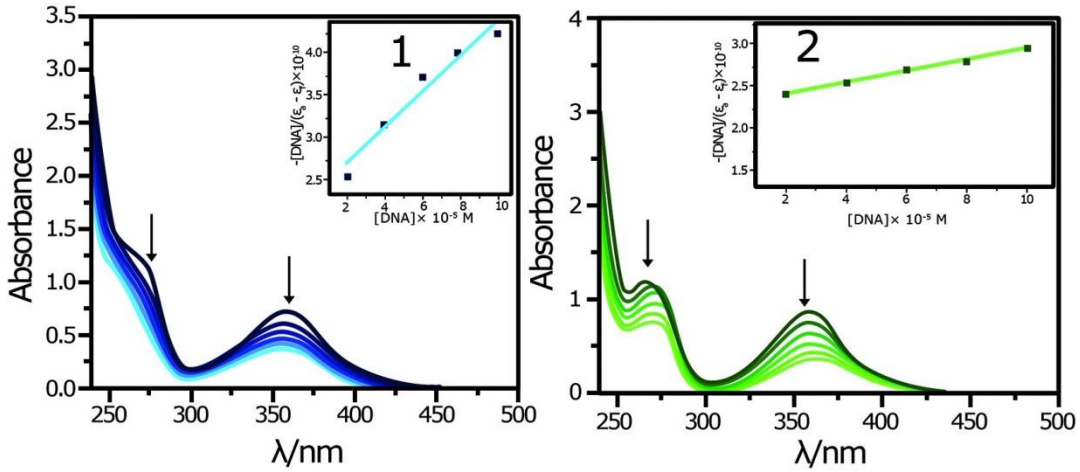

Fig. 6. UV–vis absorption spectrum of compounds **1** and **2** (1.0×10^{-5} M) in the absence and presence of CT-DNA, from 1 to 6, [DNA] = 0, 2.0×10^{-5}, 4.0×10^{-5}, 6.0×10^{-5}, $8 \times 10^{-5}$and 10×10^{-5} M, respectively. Arrows show the changes in absorbance with respect to an increase in the DNA concentration (Inset: plot between [DNA] and [DNA] / [$\varepsilon_a - \varepsilon_f$]).

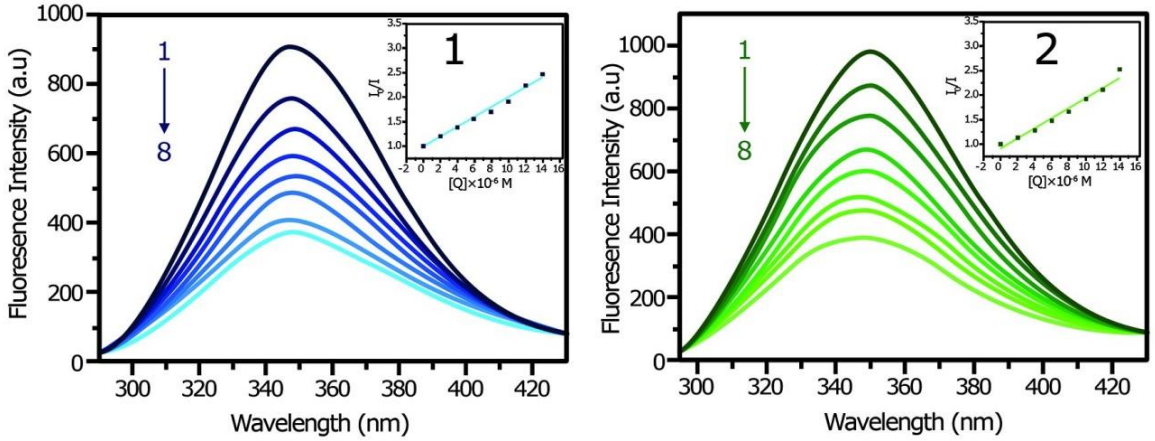

Fig. 7. Fluorescence emission spectra of BSA in the absence and presence of compounds **1** or **2**. [BSA] = 1.0×10^{-6} M, [Compound] = 0, 2.0×10^{-6} M, 4.0×10^{-6} M, 6.0×10^{-6} M, 8.0×10^{-6} M, 10.0×10^{-6} M, 12.0×10^{-6} M, 14.0×10^{-6} M, respectively; λ_{ex} =280 nm, both excitation and emission slits were 5 nm. (Inset: Plot of [Q] vs. I_0/I).

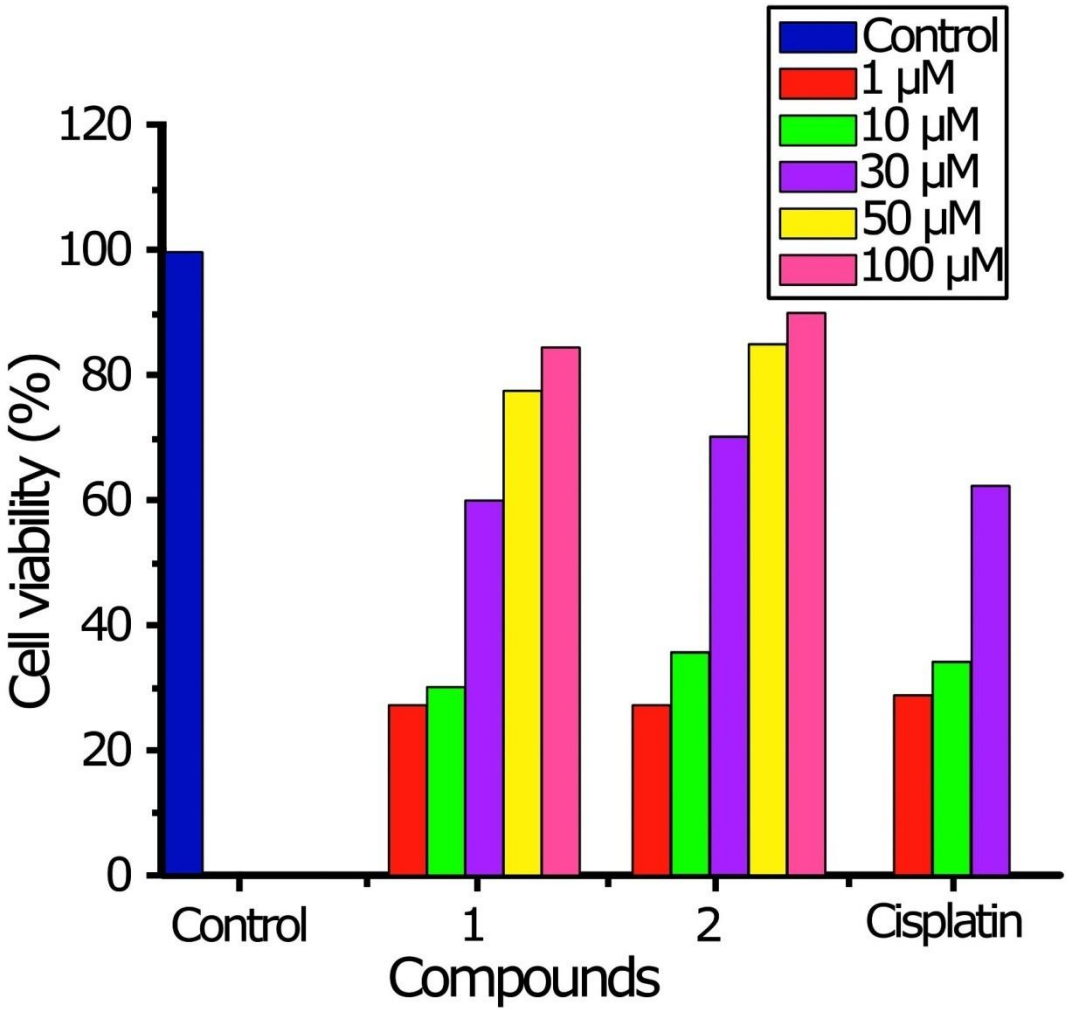

Fig. 8. In-vitro cytotoxicity of compounds **1** and **2** against HeLa tumor cells. Cytotoxicity was measured by the MTT reduction assay after 48 h. Untreated cells are used as the control.

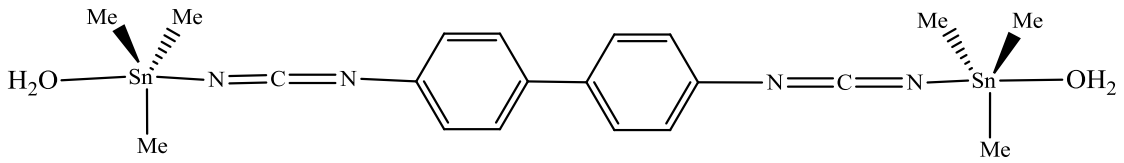

(A)

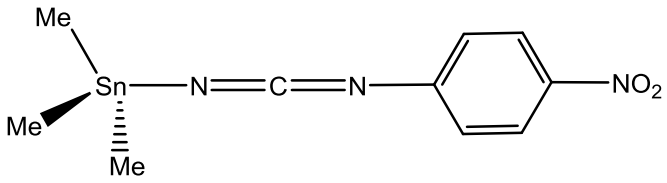

(B)

Scheme1. The structure of organotin(IV) derivatives of bpH_2 and 4-NO_2pcyd; compounds **1** (A) and **2** (B).